Novel roles of mTORC2 in regulation of insulin secretion by actin filament remodeling

Manuel Blandino-Rosano[1*], Joshua O. Scheys[2,3*], Joao Pedro Werneck-de-Castro[1], Ruy A. Louzada[1], Joana Almaça[1], Gil Leibowitz[4], Markus A. Rüegg[5], Michael N. Hall[5] and Ernesto Bernal-Mizrachi[1,6 §]

[1] Division of Endocrinology, Diabetes, and Metabolism, Department of Medicine, University of Miami Miller School of Medicine, Miami, FL

[2] Medical School, Department of Internal Medicine, Division of Metabolism, Endocrinology, and Diabetes and Brehm Center for Diabetes Research, University of Michigan. Ann Arbor, MI

[3] Current affiliation: University of Detroit Mercy School of Dentistry, Department of Biomedical and Diagnostic Sciences, Detroit, MI

[4] Diabetes Unit and Endocrine Service, Hadassah-Hebrew University Medical Center, Jerusalem, Israel.

[5] Biozentrum, University of Basel, Basel, CH-4056, Switzerland.

[6] Veterans Affairs Medical Center, Miami, Florida, USA

***indicates equal contribution.**

Disclosure Summary: The authors have nothing to disclose.

Short title: mTORC2 and insulin secretion

Keywords: mTORC2, Rictor, Insulin secretion, Actin remodeling, Incretins, GLP-1

[§]Corresponding author: Dr. Ernesto Bernal-Mizrachi

Miami VA Healthcare System and Division Endocrinology, Metabolism and Diabetes, University of Miami, 1580 NW 10th Avenue, Suite 605, Miami, FL 33136

Ph: 305-243-5631, Fax: 305-243-4039. Email: EbernalM@med.miami.edu

Supplemental Material available at https://figshare.com/s/d4c2d2f61201e42d3d0c

DOI: https://doi.org/10.6084/m9.figshare.19419896.v2

ABSTRACT

Mammalian target of rapamycin (mTOR) kinase is an essential hub where nutrients and growth factors converge to control cellular metabolism. mTOR interacts with different accessory proteins to form complexes 1 and 2 (mTORC); and each complex has different intracellular targets. Although mTORC1 role in β-cells has been extensively studied, less is known about mTORC2 function in β-cells. Here we show that mice with constitutive and inducible β-cell specific deletion of RICTOR (*βRicKO* and i*βRicKO* mice, respectively*)* are glucose intolerant due to impaired insulin secretion when glucose is injected intraperitoneally. Decreased insulin secretion in βRicKO islets was caused by abnormal actin polymerization. Interestingly, when glucose was administered orally, no difference in glucose homeostasis and insulin secretion were observed, suggesting that incretins are counteracting the mTOC2 deficiency. Mechanistically, glucagon-like peptide-1 (GLP-1), but not gastric inhibitory polypeptide (GIP), rescued insulin secretion in vivo and in vitro by improving actin polymerization in *βRicKO* islets. In conclusion, mTORC2 regulates glucose-stimulates insulin secretion by promoting actin filament remodeling.

NEW & NOTEWORTHY

The current studies uncover a novel mechanism linking mTORC2 signaling to glucose-stimulated insulin secretion by modulation of the actin filaments. This work also underscores the important role of GLP-1 on rescuing defects in insulin secretion by modulating actin polymerization and suggest that this effect is independent of mTORC2 signaling.

INTRODUCTION

The insulin-producing β-cells respond to nutrients (glucose, amino acids and fatty acids) and growth factors to adapt to different acute and chronic metabolic demands. The ability to efficiently secrete insulin, and the capacity to appropriately expand in response to increased insulin demand, are two critical factors in the pathogenesis of type 2 diabetes (T2D) (1, 2).

The Insulin-PI3-AKT signaling pathway controls cell proliferation, apoptosis, and survival in pancreatic β-cells (3-7). Overexpression of constitutively active AKT in mice specifically in β-cells leads to profound increase in β-cell mass and hyperinsulinemia (8, 9) . In addition, expression of a dominant-negative AKT resulted in impaired insulin secretion, without changes in β-cell mass (5), suggesting that AKT signaling pathway also regulates β-cell function. Two main phosphorylation sites regulate AKT kinase activity: Thr^{308} is phosphorylated by 3-phosphoinositide-dependent protein kinase 1 (PDK1); and Ser^{473} is phosphorylated by mTOR complex 2 (mTORC2), which is a multi-protein complex containing the mammalian target of rapamycin (mTOR) bound to RICTOR (rapamycin-insensitive companion of mTOR) (10). mTOR is also the catalytic component of another multi-protein complexes, the rapamycin sensitive mTOR complex 1 (mTORC1), containing the regulatory associated protein of mTOR (RAPTOR) (10). mTORC1 in β-cells controls cell size, proliferation, survival, maturation, protein translation, insulin processing and secretion, and autophagy by modulating eIF4E-binding proteins (4E-BP1, 2 and 3), ribosomal protein S6 kinases (S6K1 and 2) and Unc-51 like autophagy activating kinase (ULK1/2) among others (11-14). Less is known about the roles of mTORC2 in β-cells, but decreased mTORC2 activity in type 2 diabetic islets has been reported due to mTORC1-mediated mTORC2 inhibition (15, 16).

mTORC2 is mainly regulated by growth factors and its activity is required for normal development, as whole-body deletion of RICTOR is embryonically lethal (17, 18). mTORC2 regulates glucose uptake in adipose (19, 20) skeletal muscle (20, 21) and brown adipose (21, 22) tissues. Hepatic insulin sensitivity (23), glycolysis, and lipogenesis (22) are also regulated by mTORC2. Interestingly, hypothalamic RICTOR deletion causes impaired glucose homeostasis throughout life (24, 25). Additionally, disruption of RICTOR in endocrine precursor cells during development (*neurog3-ricKO mice*) reduced whole islet mass (26). Using mice lacking RICTOR specifically in β-cells (*βRicKO mice*) and hypothalamus, Gu et. al showed that these mice exhibit mild hyperglycemia, glucose intolerance, and poor insulin secretion caused by loss of β-cell mass, decreased β-cell proliferation, and reduced insulin content (27). In contrast, Xie and colleagues documented similar glucose excursion, insulin release, and insulin sensitivity in regular diet; but *βRicKO* mice failed to adapt normally to high fat diet (28).

mTORC2 also phosphorylates serum and glucocorticoid-inducible kinase (SGK), and protein kinase C (PKC) (18, 29). The first described mTORC2 function was to maintain normal cell cytoskeleton (30, 31) and this is done through a PKCα dependent manner (10, 32). Knockdown of RICTOR, mTOR or mLST8, but not RAPTOR, impairs the reorganization of the actin cytoskeleton network and inhibits chemotaxis and migration (31, 33). In addition, mTORC2 modulates long-term memory potentiation in the frontal cortex by regulating actin polymerization (34). In RICTOR deficient β-cells under metabolic stress, overexpression of PKCα restored the defective insulin secretion (28). Although decreased islet mass and β-mass were reported previously (26, 27), whether mTORC2 regulates cytoskeleton in β-cells was not addressed so far.

We report herein that both *βRicKO* mice and the tamoxifen inducible (i*βRicKO* mice*)* are glucose intolerant due to impaired insulin secretion when glucose is injected intraperitoneally. Although insulin content and β-cell mass are normal, *βRicKO* islets exhibit abnormal actin polymerization that resulted in decreased insulin secretion. Treatment to enhance actin polymerization reestablished insulin secretion in the *βRicKO* islets. Interestingly, glucose clearance and insulin secretion after oral glucose tolerance test are normal, suggesting that incretins rescue the secretory defect of *βRicKO* mice. We document that glucagon-like peptide-1 (GLP-1), but not gastric inhibitory polypeptide (GIP), rescues insulin secretion by improving actin polymerization in *βRicKO* islets. In conclusion, mTORC2 deficiency impairs insulin secretion due to abnormal actin polymerization. GLP-1 rescues the secretory defect induced by mTORC2 deficiency suggesting that GLP-1 acts independently of mTORC2 to promote actin polymerization and insulin secretion.

METHODS

Animals

Rictor$^{tm1.1Mnh}$ mice harboring a floxed *Rictor* allele (*Rictor*$^{f/f}$) were described previously (35). Deletion of *Rictor* in the pancreatic β-cells was achieved by intercrossing *Rictor*$^{f/f}$ mice with *Tg(Ins-cre)*^{23Herr} transgenic mice, which express Cre recombinase under the control of a rat insulin (*Ins2*) promoter (*Rip-Cre*) (36). Male offspring positive for the *Rip-Cre* transgene carrying two floxed *Rictor* alleles (*Rip-Cre*;*Rictor*$^{f/f}$) were analyzed and, for simplicity, are referred to as *βRicKO* mice. Male littermates negative for the *Rip-Cre* transgene (*Rictor*$^{f/f}$) were used as controls for all experiments. Inducible deletion of *Rictor* was achieved by crossing *Rictor*$^{f/f}$ mice with *Tg(MIP1-Cre/ERT)*^{1Lph} mice (*Mip-Cre*^{Ertm}*)*, which express Cre recombinase

under the control of a mouse insulin (*Ins1*) promoter in a tamoxifen-inducible manner (*iβRicKO* mice) (37). To exclude any effect of the *Rip-Cre* or *Mip-Cre*^{Ertm} transgene, we performed glucose tolerance test in animals harboring a floxed gene, *Mip-Cre*^{Ertm} and with *RIP-Cre* alone and no difference were observed (Supplementary Figure 1 A-B*).* (*Mip-Cre*^{Ertm}*; Rictor*$^{f/f}$) and *Rictor*$^{f/f}$ mice received three tamoxifen injections (2 mg/kg, every other day). All procedures were performed in accordance with the University Committee on the Use and Care of Animals at the University of Michigan and University of Miami.

Metabolic studies

Glucose was measured in whole blood using an AlphaTrax glucose meter (Abbott Laboratories, Alameda, CA). Plasma insulin levels were measured using a rat insulin ELISA kit (ALPCO Immunoassays). Glucose tolerance was assessed by measuring blood glucose levels following administration of 2 g/kg glucose by either intraperitoneal injection or oral gavage in overnight-fasted (16 h) mice. For an insulin tolerance test, animals fasted for 6 h received an intraperitoneal injection of either saline or human insulin (0.75 units/kg; Novolin; Novo Nordisk). *In vivo* insulin concentrations in response to a glucose load was assessed by measuring plasma insulin following 3 g/kg glucose administration by either intraperitoneal injection or oral gavage in mice that were fasted overnight for 16 h. Incretin response was determined by co-administration of 1 µmol glucagon-like peptide 1 (GLP-1) or gastric inhibitory polypeptide (GIP) with 2 g/kg glucose followed by measurement of blood glucose and plasma insulin.

Islet isolation

Islet isolation was performed as previously described (38). Briefly, the pancreas was inflated with 1 mg/mL collagenase P (Roche) injected into the common duct. Islets were handpicked and

incubated in a 37°C humidified chamber overnight in RPMI containing 10% fetal bovine serum, 1% penicillin/streptomycin and 5 mM glucose prior to performing subsequent experiments.

Islets studies

For static insulin secretion, isolated islets were incubated in Kreb's buffer (114 mM NaCL, 4.7 mM KCl, 1.2 mM KH_2PO_4, 1.16 mM $MgSO_4$, 20 mM HEPES, 2.5 mM $CaCl_2$, 25.5 mM $NaHCO_3$, and 0.2% BSA, pH 7.2) containing 2 mM glucose for 2 h. Groups of 10 islets in triplicates were incubated in Krebs-Ringer medium containing 3 mM or 24 mM glucose for 1 h (GLP-1 (25 μM) and jasplakinolide (jspk) (10 μM). Diaxozide (200 μM) and KCl (30 mM) were added when indicated. Secreted insulin was then measured in the media using by Ultrasensitive Insulin ELISA kit (ALPCO Immunoassays) and normalized to DNA content or total insulin content.

For dynamic insulin secretion, equal numbers of islets (100 islets) were handpicked and placed into chambers containing 2 mM glucose in Kreb's buffer with 100 μl Bio-Gel P-4 Media (Bio-Rad). Islets were equilibrated for 48 minutes and then perifused in intervals based on the experimental conditions. Glucose concentration was adjusted to 2mM for the first 40 minutes and then 20mM for additional 24 minutes. The perifusate was collected in an automatic fraction collector designed for a multiwell plate format. The sample container harboring the islets and the perifusion solutions were kept at 37°C in a built-in temperature-controlled chamber, and the perifusate in the collecting plate was kept at ≤ 4°C to preserve the integrity of the analytes in the perifusate. Perifusates were collected every minute. Insulin secretion was assessed by Ultrasensitive Insulin ELISA kit (ALPCO Immunoassays).

For ATP and ADP measurements, groups of 20 islets were incubated for 1 h in Krebs-Ringer containing 3mM and 24 mM, respectively, and rinsed three times in Ringer without glucose. The

samples were then processed, and ATP and ADP were measured by a luminometric method exactly as described previously (39).

Western blot

Ten to forty micrograms of protein lysate were resolved in polyacrylamide gel and transferred to a polyvinylidene fluoride membrane. The membrane was then blotted with the antibodies described in Supplementary Table 1 and visualized using an Immun-Star Western C kit (Bio-Rad). Protein band densitometry was determined by measuring pixel intensity using NIH Image J software (v1.52a (40) freely available at http://rsb.info.nih.gov/ij/index.html) and normalized to actin in the same membrane. All primary antibodies used were from Cell Signaling Technology. Goat anti-mouse and anti-rabbit secondary antibodies were from Jackson ImmunoResearch.

Immunofluorescence and morphometry

Pancreata were fixed overnight in formalin (4% formaldehyde) and embedded in paraffin as previously described (39). Antigen retrieval was achieved by boiling in Citrate Buffer (10 mM NaCitrate, pH 6.0) for 4-12 minutes. Nonspecific binding was blocked by incubating with 5% goat serum for 30 minutes and then sections were incubated at 4 ºC overnight with anti-insulin primary antibody (Dako), followed by incubation with fluorophore-conjugated secondary antibodies (Jackson Immunoresearch). Coverslips were mounted to slides using DAPI-containing mounting media (Vector Laboratories). β-cell mass assessment was performed by measuring insulin and acinar areas from five insulin-stained sections separated by 200 μM using Image Pro Software (Media Cybernetics).

Mouse insulinoma cells

Mouse insulinoma cells (MIN6) were maintained in a 37 °C humidified chamber in DMEM containing 25 mM glucose, 10% fetal bovine serum, L-glutamine and 1% penicillin/streptomycin. All cell culture reagents were purchased from Life Technologies. For filamentous actin (F-actin) experiments, cells were cultured overnight in serum-free media containing 2% BSA without glucose. Then, cells were stimulated with 10 nM Torin, or 25 μM GLP-1 with 25 mM glucose for 30 min. Cells were lysed in RIPA buffer (10 mM Tris-HCl, 1% SDS). Lysate was then resolved on polyacrylamide gel and actin polymerization was assessed as described below.

Assessment of actin polymerization

The F-actin/G-actin (globular actin) ratio was determined using an F-actin/G-actin ratio kit according to the manufacturer's instructions (Cytoskeleton). Briefly, approximately 10^6 MIN6 cells or 500 islets were lysed in actin stabilization buffer and incubated for 10 min at 37 °C. Cellular debris was removed by centrifugation at 350 x g for 5 min and insoluble F-actin was separated from soluble G-actin by centrifugation of the supernatant at 100,000 x g for 1 h. The pellet was then solubilized in depolymerization buffer for 1 h on ice. Both the soluble and insoluble fraction were resolved in a 12% polyacrylamide gel, transferred to a PVDF membrane, and then detected by immunoblot using an actin antibody.

Insulin granule dynamic in β-cells

MIN6 cells were seeded on coverslips and infected with adenoviruses containing neuropeptide Y (NPY) fused to EGFP (41). The culture medium was changed 16 h later and cells were further cultured for additional 36-48h at 37°C. Fusion of fluorescent proteins to NPY targets them to insulin granules, making them an ideal tool to monitor insulin granule dynamics in real-time

(42). Then, infected MIN6 cells are image using a confocal microscope to track insulin granules movement. Before image acquisition, MIN6 cells were incubated for 1 h with HEPES-buffered extracellular solution (125 mM NaCl, 5.9 mM KCl, 2.56 mM $CaCl_2$, 1 mM $MgCl_2$, 25 mM HEPES, 0.1% BSA) containing 3 mM glucose at 37°C. The coverslip was mounted on an imaging chamber (Warner instruments) for imaging on a Leica TCS SP5 upright laser-scanning confocal microscope (Leica Microsystems). Cells were continuously perfused with extracellular solution containing 3 mM glucose and confocal images were acquired with LAS AF software (Leica) using a 63x water immersion objective (HCX APO L 63x/0.9 NA). We used a resonance scanner for fast image acquisition to produce time-lapse recordings at 1.5 s resolution (XYT imaging). NPY-EGFP fluorescence was excited at 488 nm and emission detected at 535-550 nm. To determine changes in insulin granule dynamics, we imaged three different fields of each coverslip (5 min each movie) in the presence of high glucose concentration (25 mM), high glucose plus Torin (10 nM) and then high glucose plus Torin plus GLP-1 (25 μM). These experiments were performed in triplicate. Analysis was carried out on at least 3 independent cells and at least 10 random insulin granules. Representative movies of insulin granule movement in the three different conditions are shown as Supplementary Movies S1-3. ImageJ v1.52 and the Plug-in, MTrackJ were used to keep track of insulin EGFP granules for which end to end distance and time were measured in consecutive images. For better visualization, the series of grayscale images have been inverted using ImageJ software, and EGFP fluorescence appears in black.

Statistical analysis

Data are presented as mean ± SEM and were analysed using Prism version 9 (GraphPad Software). Mann–Whitney or unpaired t-tests were applied to compare two groups individually.

A Kruskal–Wallis test followed by Dunn's multiple comparison test were used to compare three or more groups. Two-way ANOVA was used to detect differences between groups over experimental condition followed by a Tukey (or Sidak) multiple comparison test. Differences were considered statistically significant at $p<0.05$.

RESULTS

Deletion of Rictor in pancreatic β-cells leads to reduction in Akt signaling

In order to delete *Rictor* specifically in pancreatic β-cells, *Rictor*$^{f/f}$ mice (*Rictor*$^{tm1.1Mnh}$) were crossed with *Rip-Cre* mice (*Tg(Ins-cre)*^{23Herr}) to generate *Rip-Cre;Rictor*$^{f/f}$ *(βRicKO)* mice. Islets isolated from *βRicKO* mice have significant reduction in RICTOR protein levels compared to control mice but normal protein expression of RAPTOR and mTOR (Fig 1A-B). Reduced mTORC2 activity was confirmed by decreased phosphorylation of AKT at serine 473, a known target of mTORC2 (Fig 1A and C). There was no difference in phosphorylation of AKT at threonine 308, a target of PDK1 and total Akt (Fig 1A and C). Decreased Akt activity was shown by lower levels of FoxO1 phosphorylation while phosphorylation of GSK3β was unchanged (Fig 1A and D). Total FoxO protein levels were normal (Fig 1A and D). mTORC1 activity was unaffected by loss of RICTOR since there was similar levels of ribosomal protein S6 phosphorylation in *βRicKO* islets (data not shown).

βRicKO and iβRicKO mice are glucose intolerant and exhibit impaired insulin secretion with normal β-cell mass and insulin content.

Body weight, fed and fasting glucose, fed and fasting insulin were within the normal range and not different from controls (Fig 2A-C). However, glucose tolerance was impaired in both, males (Fig 2D-E) and females (Supplementary Figure 1 C-D) *βRicKO* mice. Glucose intolerance in *βRicKO* mice was likely due to impaired insulin secretion *in vivo* (Fig 2F). No differences in

insulin sensitivity between *βRicKO* and control mice were oserved (Fig 2G). Despite the defect in glucose-induced insulin secretion *in vivo*, β-cell mass was similar in *βRicKO* and control mice (Fig 2 H).

To eliminate the maturation effects that arise from loss of RICTOR during β-cell development, we disrupted RICTOR in adult β-cells by crossing the *floxed-Rictor* model with mice expressing a tamoxifen-inducible *Cre* under the control of the mouse *Ins1* promoter (*Mip-Cre*^{Ertm}). Before tamoxifen treatment, i*βRicKO* mice were normoglycemic and exhibit normal glucose tolerance (Supp Fig 1 E-F). Similar to *βRicKO* mice, the i*βRicKO* mice had impaired glucose clearance after three weeks of tamoxifen injection (Fig 3A-B). In vivo glucose-stimulated insulin secretion was also impaired in i*βRicKO* mice (Fig 3C). Examination of fasting and fed glucose and insulin levels showed comparable levels in i*βRicKO* and control mice (Fig 3D and E). There was no difference in β-cell mass suggesting that the alterations in glucose tolerance in i*βRicKO* mice resulted from an insulin secretory defect (Fig 3F).

Impaired insulin secretion in the βRicKO mice is associated with alterations in polymerization of actin filaments.

To further characterize the alteration in insulin secretion in *βRicKO* mice, we performed in vitro studies. Isolated islets from *βRicKO* mice secreted less insulin following stimulation with high glucose (20 mM) or 30 mM KCl (Fig 4A), suggesting a defect that is distal to plasma membrane depolarization and calcium influx. In an attempt to explain the defect in insulin secretion, we assessed insulin content of islets. Insulin content per islet was similar in *βRicKO* and control mice (Fig 4B). Additionally, the ATP/ADP ratio was not different in *βRicKO* islets, suggesting that glucose metabolism was preserved (Fig 4C). To further investigate the defect in insulin secretion from βRicKO mice, isolated islets perifusion studies were performed with low (2G)

and high (20G) glucose. Interestingly, both phases of insulin secretion are disrupted in βRicKO islets (Supp Fig 2 A-B).

Altogether the insulin secretion in vitro suggests that distal events to calcium influx play a role in the insulin secretory defect in *βRicKO* mice. Normal cytoskeleton architecture plays an important role in late events of insulin secretion (43). In MIN6 cells, the acute transition from no glucose to high glucose levels (0 to 25 mM glucose) increases the F-actin/G-actin ratio enabling insulin granule exocytosis (Fig 4D). Treatment with the mTORC1/mTORC2 inhibitor, Torin, reduced glucose-induced actin polymerization in MIN6 cells (Fig 4D). We then assessed F-actin/G-actin ratio in islets isolated from *βRicKO* and control mice. F-/G-actin ratio was reduced in *βRicKO* islets (Fig 4E). Remarkably, treatment of isolated islets with jasplakinolide (jspk), a pharmacological inducer of actin polymerization, restored insulin secretion in *βRicKO* islets to levels similar to those of control islets (Fig 4F).

Glucagon-like peptide 1 restores insulin secretion by normalizing actin filament polymerization.

To assess whether the defects in glucose tolerance observed in *βRicKO* mice were rescued by incretin signaling, we performed oral tolerance test (oGTT). Remarkably, there was no difference between *βRicKO* and control mice in glucose clearance during the oGTT (Fig 5A-B) which is in stark contrast to the result of glucose delivered intraperitoneally (Fig 2D-E and Fig 3A-B). Also, insulin secretion in *βRicKO* mice was normalized in the oGTT (Fig 5C), suggesting that incretins were involved. To further evaluate the incretin effect, we co-administered glucose with GLP-1 by intraperitoneal injections. Glucose tolerance was restored to normal levels in *βRicKO* mice after GLP1 injection (Fig 5D-E) and this was accompanied by a similar GSIS (Figure 5F). In contrast, co-injection of glucose with glucose-dependent insulinotropic peptide

(GIP) had little effect on the impaired glucose tolerance observed in *βRicKO* mice (Fig 5G-H). This was associated with a decreased GSIS in *βRicKO* mice (Figure 5I).

We then assessed if the normalization of insulin secretion of *βRicKO* mice by GLP-1 in vivo was validated in islets in vitro. GLP1 treatment rescued the insulin secretory defect in *βRicKO* islets *in vitro* (Fig 6A). Given the defect on actin filament assembling and insulin secretion in *βRicKO* islets, we hypothesize that GLP-1 could restore insulin secretion in *βRicKO* islets by increasing F-actin dynamics. The better insulin secretion in *βRicKO* islets treated with GLP-1 was associated with a F-actin/G-actin ratio compared to control (Fig 6B). In MIN6 cells, high glucose levels induced F-actin/G-actin ratio compared to low glucose and co-culture with high glucose and GLP-1 further increased F-actin/G-actin ratio in MIN6 cells (Fig 6C). Taken together, these studies support the concept that GLP-1 regulates actin polymerization independent of mTORC2 and normalizes the defect in insulin secretion observed in *βRicKO* islets.

mTORC2 regulates insulin granule dynamic in β-cells

To determine the effect of mTORC2 on insulin granule dynamics, we infected MIN6 cells with adenoviruses encoding neuropeptide Y (NPY) fused to EGFP. NPY-EGFP fluorescence can be detected in the cytoplasm of the cells, in different compartments of the secretory pathway (ER, Golgi) as well as in secretory granules that appear as individual fluorescent dots. Increasing extracellular glucose concentration triggered secretory granule movement and the appearance of new granules (Movie S1 and Fig 6D). Insulin granule movement was inhibited by application of the mTOR inhibitor Torin (Movie S2 and Fig 6D). Interestingly, GLP-1 rescued secretory granule movement and increased the density of granules close or at the plasma membrane (Movie S3 and Fig 6D).

DISCUSSION

Extensive work has shown a key role of mTORC1 and downstream targets in β-cells (11-14, 16, 26-28, 44). In the present study, we report that mice with mTORC2-deficient β-cells (*βRicKO* mice*)* exhibit glucose intolerance after the ipGTT due to reduced glucose-stimulated insulin secretion both in vivo and in vitro, although fasting and non-fasting glycemia and insulinemia are normal. Loss of RICTOR did not affect islet insulin content, β-cell mass, or ATP/ADP ratio. The alterations in glucose intolerance is caused by a defect in insulin secretion, but not β-cell mass and insulin sensitivity. The mechanism behind the altered insulin secretion is caused by abnormal actin polymerization and restoring actin polymerization improved insulin secretion of *βRicKO* islets. Remarkably, changes in glucose tolerance in response to oral glucose (oGTT) and insulin secretion were normal in the *βRicKO* mice*,* indicating that incretins were involved. GLP-1 treatment in vivo and in vitro restored the secretory defect by improving actin polymerization. This study discovers a previously unidentified mechanism for mTORC2 signaling in insulin secretion by altering actin remodeling.

Previous studies aimed to assess mTORC2 role in β-cells with conflicting results (27, 28). Gu *et al*. observed that the *βRicKO* mice were mildly hyperglycemic (~130-140 mg/dl) and glucose intolerant after intraperitoneal glucose (27). These studies attributed the diminished insulin secretory responses and impaired glucose tolerance in *βRicKO* mice to 30% reduction in β-cell mass (27). This phenotype is inconsistent with similar studies using the same mouse model in standard diet (28). We confirmed that *βRicKO* mice are intolerant to glucose after intraperitoneal GTT due to reduced insulin secretion. However, the defect in insulin secretion was not accompanied by alteration in β-cell mass in both newborn (data not shown) and adult *βRicKO* mice, indicating that β-cell function is predominantly affected. In line with our findings, Xie et al

316 also did not observe difference in β-cell mass but they found a 50% reduction in insulin content
317 in the *βRicKO* islets (28). Our studies extend these observations by identifying a novel role of
318 mTORC2 in insulin secretion by altering actin remodeling. The differences between our study
319 and Gu *et al*. results can be partially explained by different Cre-recombinase mouse models used
320 to disrupt mTORC2 signaling. The Ins2-cre$^{25Mgn/J}$ used by Gu *et al*. has been shown to have
321 hypothalamic expression and alterations in glucose homeostasis (27, 45, 46). Our studies and
322 those by *Xie et al* used Ins2-cre^{23Herr} (13, 28, 36). It is possible that ectopic expression in the
323 brain using this RIP-cre could result in altered metabolism (37). However, there are several lines
324 of evidence suggesting that this is unlikely: a) non-fasting glycemia and plasma insulin are
325 normal; b) the mechanism for the impaired insulin secretion is intrinsic to the β-cells as *βRicKO*
326 mice exhibit similar insulin sensitivity as control mice in this model and in a previous
327 publication (28); c) the impaired insulin secretion and glucose intolerance was confirmed by
328 Rictor deletion in tamoxifen inducible deletion in adult mice after crossing with a different cre-
329 recombinase mouse (the *MIP-cre* mouse).

330 A normal and dynamic cellular cytoskeleton (actin and tubulin microtubules) is essential for β-
331 cell function and insulin secretion (47-49). F-actin can both favor or impede insulin secretion
332 depending on cellular localization and interaction with other proteins (47). Actin filaments in
333 proximity to the cell membrane can act as physical barrier for insulin secretion and increasing
334 glucose levels stimulate localized depolymerization of actin, allowing access of insulin granules
335 to the cell periphery for exocytosis (50-52). On the other hand, glucose also stimulates the
336 polymerization of F-actin to serve as a track for insulin granule trafficking to replenish the
337 readily releasable pool (49, 53). For example, β-catenin and secretagogin sustain insulin
338 secretion by maintaining cellular F-actin fraction and insulin secretion (43, 54). mTORC2 was

first identified as a regulator of cytoskeleton structure and RICTOR deletion resulted in altered actin polymerization (30, 34). This is the first evidence that link mTORC2 to actin filaments as a mechanism underlying the defective insulin secretion. The conclusion that *βRicKO* islets exhibit a decrease in F-actin polymerization was supported by decrease in actin remodeling in *βRicKO* islets and MIN6 cells treated with Torin. In addition, treatment with jasplakinolide, an actin filament polymerizing agent, restored insulin secretion in *βRicKO* islets indicating that this mechanism is involved in the insulin secretory defect observed by reduced mTORC2 activity. Noteworthy, our studies are limited to total content of F- and G-actin in the cell. Nevertheless, a negative effect on insulin secretion (55-58) was reported using jasplakinolide, and more studies are needed to uncover the effects of actin remodeling agents on vesicle movement and insulin secretion. The regulation of actin polymerization in different cell compartments e.g. cortical *vs* central by mTORC2 is yet to be determined. An interesting finding in our studies was the GLP-1 rescue of the insulin secretory defect observed in *βRicKO* islets and mice. GLP-1 stimulates/amplifies insulin secretion via cAMP pathway (59). Interestingly, GLP-1 restores actin filament structure in βRicKO islets and improves insulin secretion in vivo and in vitro. Consistent with our findings, previous work has shown that Exendin-4 (Ex-4), a GLP-1 analogue used to treat diabetes, increases F/G actin ratio (60). Given the rapid effects of GLP-1 on rescuing the secretory defects of βRicKO islets, it is likely that the actin remodeling mechanism predominates over cAMP/PKA/CREB-mediated transcriptional regulation of key genes such as IRS2 (61). However, actin in excess, as observed in high-glucose treated INS-1 β-cells (glucotoxicity), delayed insulin granules mobilization. In this scenario, GLP-1 depolymerized F-actin and restored insulin secretion (60, 62). We did not assess F-actin in different cell compartments, but we show that granules movement in mouse insulinoma cells β-cells (MIN-6)

362 treated with torin decreased insulin granules movement. Importantly, GLP-1 was able to restore
363 granules movement to controls values.
364 mTORC2 can regulate insulin secretion by acting on multiple downstream targets but the most
365 well characterized target is AKT. However, mTORC2 also phosphorylates similar AGC kinases,
366 namely SGK and PKC (18, 29). It has been shown that HFD enhances mTORC2/PKC proteins
367 levels in control but not in *βRicKO* islets suggesting that mTORC-PKCα pathway is involved in
368 metabolic stress adaptation (28). Overexpressing PKCα restored the defective GSIS in *βRicKO*
369 islets (28). Our results together with previous studies indicate that β-cell mTORC2 regulates
370 insulin secretion but not β-mass during normal conditions and after HFD administration (data not
371 shown). How mTORC2 regulates insulin secretion is partially understood but Akt signaling and
372 SGK could be involved. mTORC2 could regulate distal events of insulin secretion by activating
373 Akt as full activation of this kinase is required for this process (5). Alternatively, mTORC2
374 could modulate insulin secretion by regulating actin polymerization. Consistent with our results
375 linking mTORC2 to actin polymerization, mTORC2 regulates actin polymerization in CA1
376 neurons by increase in Rac1-GTPase activity and phosphorylation of PAK and Cofilin through
377 the Rac1-specific guanine nucleotide-exchange factor (GEF) Tiam1 (34). All these Rho family
378 of GTPases, effectors and GEFs are important for glucose-stimulated insulin secretion *in vivo*
379 and *in vitro* in mouse β-cells (47, 48, 51, 63-65). We cannot rule out that actin modulation by
380 RICTOR may be independent of mTORC2 activity because depletion of RICTOR in neutrophils
381 impairs actin polymerization, and therefore chemotaxis, while depletion of another critical
382 mTORC2 component, SIN1, has no effect (66). Similarly, RICTOR associates with and inhibits
383 Rho-GDP dissociation inhibitor 2 (RhoGDI2) and *Rictor*-deficient fibroblasts have impaired cell
384 migration due to reduced Rac and Cdc42 GTPase activity, independently of mTORC2 activity

(67). These small GTPases are known to play a role in insulin secretion by modulation of actin dynamics (48) and a recent study has demonstrated that knocking down expression of *RhoGDI* in β-cells improves 2nd phase secretion (68). In the present study, it appears that the effects of RICTOR deficiency on actin polymerization are mTORC2-dependent because Torin treatment *in vitro* reduces formation of F-actin and reduces insulin granules movement. However, further studies are needed to reveal the precise mechanisms.

In summary, the current studies uncover a novel mechanism linking mTORC2 signaling to glucose-stimulated insulin secretion by modulation of the actin filaments. This work also underscores the important role of GLP-1 on rescuing defects in insulin secretion by modulating actin polymerization and suggest that this effect is independent of mTORC2 signaling.

Acknowledgements

The authors are grateful to Burton Wice (Washington University, St. Louis) for providing purified GLP-1 and GIP.

Funding

This work was supported by grants from the National Institutes of Health R01-DK084236 and R01-DK073716 (to EBM) and by the Training Grant T32-DK071212 Developmental Origins of Endocrine Dysfunctions (to JOS).

Conflict of Interest

No potential conflicts of interest relevant to this article were reported.

Author contribution

JOS and MBR designed and performed experiments, analyzed the data, contributed to discussion, and wrote the manuscript. JPW, RAL and GL contributed to discussion, and wrote the manuscript. JA designed and performed experiments. MR, and MH generated mice. EBM directed the project, contributed to discussion, and edited the manuscript. EBM is the guarantor of this work and, as such, had full access to all the data in the study and takes responsibility for the integrity of the data and the accuracy of the data analysis.

Data availability statement

All data supporting the results in the paper are in the body of the manuscript.

References

1. **Alejandro EU, Gregg B, Blandino-Rosano M, Cras-Meneur C, and Bernal-Mizrachi E**. Natural history of beta-cell adaptation and failure in type 2 diabetes. *Mol Aspects Med* 42: 19-41, 2015.

2. **Arvan P, Bernal-Mizrachi E, Liu M, Pietropaolo M, Satin L, Schnell S, and Soleimanpour SA**. Molecular aspects of pancreatic beta cell failure and diabetes. *Mol Aspects Med* 42: 1-2, 2015.

3. **Jetton TL, Lausier J, LaRock K, Trotman WE, Larmie B, Habibovic A, Peshavaria M, and Leahy JL**. Mechanisms of compensatory beta-cell growth in insulin-resistant rats: roles of Akt kinase. *Diabetes* 54: 2294-2304, 2005.

4. **Elghazi L, Rachdi L, Weiss AJ, Cras-Meneur C, and Bernal-Mizrachi E**. Regulation of beta-cell mass and function by the Akt/protein kinase B signalling pathway. *Diabetes Obes Metab* 9 Suppl 2: 147-157, 2007.

5. **Bernal-Mizrachi E, Fatrai S, Johnson JD, Ohsugi M, Otani K, Han Z, Polonsky KS, and Permutt MA**. Defective insulin secretion and increased susceptibility to experimental diabetes are induced by reduced Akt activity in pancreatic islet beta cells. *J Clin Invest* 114: 928-936, 2004.

6. **Jara MA, Werneck-De-Castro JP, Lubaczeuski C, Johnson JD, and Bernal-Mizrachi E**. Pancreatic and duodenal homeobox-1 (PDX1) contributes to beta-cell mass expansion and proliferation induced by Akt/PKB pathway. *Islets* 12: 32-40, 2020.

7. **Blandino-Rosano M, Alejandro EU, Sathyamurthy A, Scheys JO, Gregg B, Chen AY, Rachdi L, Weiss A, Barker DJ, Gould AP, Elghazi L, and Bernal-Mizrachi E**. Enhanced beta cell proliferation in mice overexpressing a constitutively active form of Akt and one allele of p21Cip. *Diabetologia* 55: 1380-1389, 2012.

8. **Bernal-Mizrachi E, Wen W, Stahlhut S, Welling CM, and Permutt MA**. Islet beta cell expression of constitutively active Akt1/PKB alpha induces striking hypertrophy, hyperplasia, and hyperinsulinemia. *J Clin Invest* 108: 1631-1638, 2001.

9. **Tuttle RL, Gill NS, Pugh W, Lee JP, Koeberlein B, Furth EE, Polonsky KS, Naji A, and Birnbaum MJ**. Regulation of pancreatic beta-cell growth and survival by the serine/threonine protein kinase Akt1/PKBalpha. *Nat Med* 7: 1133-1137, 2001.

10. **Liu GY, and Sabatini DM**. mTOR at the nexus of nutrition, growth, ageing and disease. *Nat Rev Mol Cell Biol* 21: 183-203, 2020.

11. **Yin Q, Ni Q, Wang Y, Zhang H, Li W, Nie A, Wang S, Gu Y, Wang Q, and Ning G**. Raptor determines beta-cell identity and plasticity independent of hyperglycemia in mice. *Nat Commun* 11: 2538, 2020.

12. **Wang Y, Sun J, Ni Q, Nie A, Gu Y, Wang S, Zhang W, Ning G, Wang W, and Wang Q**. Dual Effect of Raptor on Neonatal beta-Cell Proliferation and Identity Maintenance. *Diabetes* 68: 1950-1964, 2019.

13. **Blandino-Rosano M, Barbaresso R, Jimenez-Palomares M, Bozadjieva N, Werneck-de-Castro JP, Hatanaka M, Mirmira RG, Sonenberg N, Liu M, Ruegg MA, Hall MN, and Bernal-Mizrachi E**. Loss of mTORC1 signalling impairs beta-cell homeostasis and insulin processing. *Nat Commun* 8: 16014, 2017.

14. **Ni Q, Gu Y, Xie Y, Yin Q, Zhang H, Nie A, Li W, Wang Y, Ning G, Wang W, and Wang Q**. Raptor regulates functional maturation of murine beta cells. *Nat Commun* 8: 15755, 2017.

15. **Yuan T, Rafizadeh S, Gorrepati KD, Lupse B, Oberholzer J, Maedler K, and Ardestani A**. Reciprocal regulation of mTOR complexes in pancreatic islets from humans with type 2 diabetes. *Diabetologia* 60: 668-678, 2017.

16. **Yuan T, Lupse B, Maedler K, and Ardestani A**. mTORC2 Signaling: A Path for Pancreatic beta Cell's Growth and Function. *J Mol Biol* 430: 904-918, 2018.

17. **Shiota C, Woo JT, Lindner J, Shelton KD, and Magnuson MA**. Multiallelic disruption of the rictor gene in mice reveals that mTOR complex 2 is essential for fetal growth and viability. *Dev Cell* 11: 583-589, 2006.

18. **Guertin DA, Stevens DM, Thoreen CC, Burds AA, Kalaany NY, Moffat J, Brown M, Fitzgerald KJ, and Sabatini DM**. Ablation in mice of the mTORC components raptor, rictor, or mLST8 reveals that mTORC2 is required for signaling to Akt-FOXO and PKCalpha, but not S6K1. *Dev Cell* 11: 859-871, 2006.

19. **Cybulski N, and Hall MN**. TOR complex 2: a signaling pathway of its own. *Trends Biochem Sci* 34: 620-627, 2009.

20. **Yu D, Tomasiewicz JL, Yang SE, Miller BR, Wakai MH, Sherman DS, Cummings NE, Baar EL, Brinkman JA, Syed FA, and Lamming DW**. Calorie-Restriction-Induced Insulin Sensitivity Is Mediated by Adipose mTORC2 and Not Required for Lifespan Extension. *Cell Rep* 29: 236-248 e233, 2019.

21. **Jung SM, Hung CM, Hildebrand SR, Sanchez-Gurmaches J, Martinez-Pastor B, Gengatharan JM, Wallace M, Mukhopadhyay D, Martinez Calejman C, Luciano AK, Hsiao WY, Tang Y, Li H, Daniels DL, Mostoslavsky R, Metallo CM, and Guertin DA**. Non-canonical mTORC2 Signaling Regulates Brown Adipocyte Lipid Catabolism through SIRT6-FoxO1. *Mol Cell* 75: 807-822 e808, 2019.

22. **Hung CM, Calejman CM, Sanchez-Gurmaches J, Li H, Clish CB, Hettmer S, Wagers AJ, and Guertin DA**. Rictor/mTORC2 loss in the Myf5 lineage reprograms brown fat metabolism and protects mice against obesity and metabolic disease. *Cell Rep* 8: 256-271, 2014.

23. **Lamming DW, Ye L, Katajisto P, Goncalves MD, Saitoh M, Stevens DM, Davis JG, Salmon AB, Richardson A, Ahima RS, Guertin DA, Sabatini DM, and Baur JA**. Rapamycin-induced insulin resistance is mediated by mTORC2 loss and uncoupled from longevity. *Science* 335: 1638-1643, 2012.

24. **Kocalis HE, Hagan SL, George L, Turney MK, Siuta MA, Laryea GN, Morris LC, Muglia LJ, Printz RL, Stanwood GD, and Niswender KD**. Rictor/mTORC2 facilitates central regulation of energy and glucose homeostasis. *Mol Metab* 3: 394-407, 2014.

25. **Chellappa K, Brinkman JA, Mukherjee S, Morrison M, Alotaibi MI, Carbajal KA, Alhadeff AL, Perron IJ, Yao R, Purdy CS, DeFelice DM, Wakai MH, Tomasiewicz J, Lin A, Meyer E, Peng Y, Arriola Apelo SI, Puglielli L, Betley JN, Paschos GK, Baur JA, and Lamming DW**. Hypothalamic mTORC2 is essential for metabolic health and longevity. *Aging Cell* 18: e13014, 2019.

26. **Sinagoga KL, Stone WJ, Schiesser JV, Schweitzer JI, Sampson L, Zheng Y, and Wells JM**. Distinct roles for the mTOR pathway in postnatal morphogenesis, maturation and function of pancreatic islets. *Development* 144: 2402-2414, 2017.

27. **Gu Y, Lindner J, Kumar A, Yuan W, and Magnuson MA**. Rictor/mTORC2 is essential for maintaining a balance between beta-cell proliferation and cell size. *Diabetes* 60: 827-837, 2011.

28. **Xie Y, Cui C, Nie A, Wang Y, Ni Q, Liu Y, Yin Q, Zhang H, Li Y, Wang Q, Gu Y, and Ning G**. The mTORC2/PKC pathway sustains compensatory insulin secretion of pancreatic beta cells in response to metabolic stress. *Biochim Biophys Acta Gen Subj* 1861: 2039-2047, 2017.

29. **Garcia-Martinez JM, and Alessi DR**. mTOR complex 2 (mTORC2) controls hydrophobic motif phosphorylation and activation of serum- and glucocorticoid-induced protein kinase 1 (SGK1). *Biochem J* 416: 375-385, 2008.

30. **Sarbassov DD, Ali SM, Kim DH, Guertin DA, Latek RR, Erdjument-Bromage H, Tempst P, and Sabatini DM**. Rictor, a novel binding partner of mTOR, defines a rapamycin-insensitive and raptor-independent pathway that regulates the cytoskeleton. *Curr Biol* 14: 1296-1302, 2004.

31. **Jacinto E, Loewith R, Schmidt A, Lin S, Ruegg MA, Hall A, and Hall MN**. Mammalian TOR complex 2 controls the actin cytoskeleton and is rapamycin insensitive. *Nat Cell Biol* 6: 1122-1128, 2004.

32. **Larsson C**. Protein kinase C and the regulation of the actin cytoskeleton. *Cell Signal* 18: 276-284, 2006.

33. **Liu L, Das S, Losert W, and Parent CA**. mTORC2 regulates neutrophil chemotaxis in a cAMP- and RhoA-dependent fashion. *Dev Cell* 19: 845-857, 2010.

34. **Huang W, Zhu PJ, Zhang S, Zhou H, Stoica L, Galiano M, Krnjevic K, Roman G, and Costa-Mattioli M**. mTORC2 controls actin polymerization required for consolidation of long-term memory. *Nature neuroscience* 16: 441-448, 2013.

35. **Bentzinger CF, Romanino K, Cloetta D, Lin S, Mascarenhas JB, Oliveri F, Xia J, Casanova E, Costa CF, Brink M, Zorzato F, Hall MN, and Ruegg MA**. Skeletal muscle-specific ablation of raptor, but not of rictor, causes metabolic changes and results in muscle dystrophy. *Cell Metab* 8: 411-424, 2008.

36. **Herrera PL**. Adult insulin- and glucagon-producing cells differentiate from two independent cell lineages. *Development* 127: 2317-2322, 2000.

37. **Wicksteed B, Brissova M, Yan W, Opland DM, Plank JL, Reinert RB, Dickson LM, Tamarina NA, Philipson LH, Shostak A, Bernal-Mizrachi E, Elghazi L, Roe MW, Labosky PA, Myers MG, Jr., Gannon M, Powers AC, and Dempsey PJ**. Conditional gene targeting in mouse pancreatic ss-Cells: analysis of ectopic Cre transgene expression in the brain. *Diabetes* 59: 3090-3098, 2010.

38. **Werneck-de-Castro JP, Blandino-Rosano M, Hilfiker-Kleiner D, and Bernal-Mizrachi E**. Glucose stimulates microRNA-199 expression in murine pancreatic beta-cells. *J Biol Chem* 295: 1261-1270, 2020.

39. **Elghazi L, Balcazar N, Blandino-Rosano M, Cras-Meneur C, Fatrai S, Gould AP, Chi MM, Moley KH, and Bernal-Mizrachi E**. Decreased IRS signaling impairs beta-cell cycle progression and survival in transgenic mice overexpressing S6K in beta-cells. *Diabetes* 59: 2390-2399, 2010.

40. **Schneider CA, Rasband WS, and Eliceiri KW**. NIH Image to ImageJ: 25 years of image analysis. *Nature methods* 9: 671-675, 2012.

41. **Zhu D, Zhang Y, Lam PP, Dolai S, Liu Y, Cai EP, Choi D, Schroer SA, Kang Y, Allister EM, Qin T, Wheeler MB, Wang CC, Hong WJ, Woo M, and Gaisano HY**. Dual role of VAMP8 in regulating insulin exocytosis and islet beta cell growth. *Cell Metab* 16: 238-249, 2012.

42. **Almaca J, Liang T, Gaisano HY, Nam HG, Berggren PO, and Caicedo A**. Spatial and temporal coordination of insulin granule exocytosis in intact human pancreatic islets. *Diabetologia* 58: 2810-2818, 2015.

43. **Sorrenson B, Cognard E, Lee KL, Dissanayake WC, Fu Y, Han W, Hughes WE, and Shepherd PR**. A Critical Role for beta-Catenin in Modulating Levels of Insulin Secretion from beta-Cells by Regulating Actin Cytoskeleton and Insulin Vesicle Localization. *J Biol Chem* 291: 25888-25900, 2016.

44. **Alejandro EU, Bozadjieva N, Blandino-Rosano M, Wasan MA, Elghazi L, Vadrevu S, Satin L, and Bernal-Mizrachi E**. Overexpression of Kinase-Dead mTOR Impairs Glucose Homeostasis by Regulating Insulin Secretion and Not beta-Cell Mass. *Diabetes* 66: 2150-2162, 2017.

45. **Pomplun D, Florian S, Schulz T, Pfeiffer AF, and Ristow M**. Alterations of pancreatic beta-cell mass and islet number due to Ins2-controlled expression of Cre recombinase: RIP-Cre revisited; part 2. *Horm Metab Res* 39: 336-340, 2007.

46. **Lee JY, Ristow M, Lin X, White MF, Magnuson MA, and Hennighausen L**. RIP-Cre revisited, evidence for impairments of pancreatic beta-cell function. *J Biol Chem* 281: 2649-2653, 2006.

47. **Kalwat MA, and Thurmond DC**. Signaling mechanisms of glucose-induced F-actin remodeling in pancreatic islet beta cells. *Exp Mol Med* 45: e37, 2013.

48. **Wang Z, and Thurmond DC**. Mechanisms of biphasic insulin-granule exocytosis - roles of the cytoskeleton, small GTPases and SNARE proteins. *J Cell Sci* 122: 893-903, 2009.

49. **Orci L, Gabbay KH, and Malaisse WJ**. Pancreatic beta-cell web: its possible role in insulin secretion. *Science* 175: 1128-1130, 1972.

50. **Thurmond DC, Gonelle-Gispert C, Furukawa M, Halban PA, and Pessin JE**. Glucose-stimulated insulin secretion is coupled to the interaction of actin with the t-SNARE (target membrane soluble N-ethylmaleimide-sensitive factor attachment protein receptor protein) complex. *Mol Endocrinol* 17: 732-742, 2003.

51. **Nevins AK, and Thurmond DC**. Glucose regulates the cortical actin network through modulation of Cdc42 cycling to stimulate insulin secretion. *Am J Physiol Cell Physiol* 285: C698-710, 2003.

52. **Jewell JL, Luo W, Oh E, Wang Z, and Thurmond DC**. Filamentous actin regulates insulin exocytosis through direct interaction with Syntaxin 4. *J Biol Chem* 283: 10716-10726, 2008.

53. **Heaslip AT, Nelson SR, Lombardo AT, Beck Previs S, Armstrong J, and Warshaw DM**. Cytoskeletal dependence of insulin granule movement dynamics in INS-1 beta-cells in response to glucose. *PLoS One* 9: e109082, 2014.

54. **Yang SY, Lee JJ, Lee JH, Lee K, Oh SH, Lim YM, Lee MS, and Lee KJ**. Secretagogin affects insulin secretion in pancreatic beta-cells by regulating actin dynamics and focal adhesion. *Biochem J* 473: 1791-1803, 2016.

55. **Shawl AI, Park KH, Kim BJ, Higashida C, Higashida H, and Kim UH**. Involvement of actin filament in the generation of Ca2+ mobilizing messengers in glucose-induced Ca2+ signaling in pancreatic beta-cells. *Islets* 4: 145-151, 2012.

56. **Tsuboi T, da Silva Xavier G, Leclerc I, and Rutter GA**. 5'-AMP-activated protein kinase controls insulin-containing secretory vesicle dynamics. *J Biol Chem* 278: 52042-52051, 2003.

57. **Wilson JR, Ludowyke RI, and Biden TJ**. A redistribution of actin and myosin IIA accompanies Ca(2+)-dependent insulin secretion. *FEBS Lett* 492: 101-106, 2001.

58. **Lawrence JT, and Birnbaum MJ**. ADP-ribosylation factor 6 regulates insulin secretion through plasma membrane phosphatidylinositol 4,5-bisphosphate. *Proc Natl Acad Sci U S A* 100: 13320-13325, 2003.

59. **Muller TD, Finan B, Bloom SR, D'Alessio D, Drucker DJ, Flatt PR, Fritsche A, Gribble F, Grill HJ, Habener JF, Holst JJ, Langhans W, Meier JJ, Nauck MA, Perez-Tilve D, Pocai A, Reimann F, Sandoval DA, Schwartz TW, Seeley RJ, Stemmer K, Tang-Christensen M, Woods SC, DiMarchi RD, and Tschop MH**. Glucagon-like peptide 1 (GLP-1). *Mol Metab* 30: 72-130, 2019.

60. **Zhao F, Li J, Wang R, Xu H, Ma K, Kong X, Sun Z, Niu X, Jiang J, Liu B, Li B, Duan F, and Chen X**. Exendin-4 promotes actin cytoskeleton rearrangement and protects cells from Nogo-A-Delta20 mediated spreading inhibition and growth cone collapse by down-regulating RhoA expression and activation via the PI3K pathway. *Biomed Pharmacother* 109: 135-143, 2019.

61. **Jhala US, Canettieri G, Screaton RA, Kulkarni RN, Krajewski S, Reed J, Walker J, Lin X, White M, and Montminy M**. cAMP promotes pancreatic beta-cell survival via CREB-mediated induction of IRS2. *Genes Dev* 17: 1575-1580, 2003.

62. **Quinault A, Gausseres B, Bailbe D, Chebbah N, Portha B, Movassat J, and Tourrel-Cuzin C**. Disrupted dynamics of F-actin and insulin granule fusion in INS-1 832/13 beta-cells exposed to glucotoxicity: partial restoration by glucagon-like peptide 1. *Biochim Biophys Acta* 1862: 1401-1411, 2016.

63. **Kowluru A**. Small G proteins in islet beta-cell function. *Endocr Rev* 31: 52-78, 2010.

64. **Asahara S, Shibutani Y, Teruyama K, Inoue HY, Kawada Y, Etoh H, Matsuda T, Kimura-Koyanagi M, Hashimoto N, Sakahara M, Fujimoto W, Takahashi H, Ueda S, Hosooka T, Satoh T, Inoue H, Matsumoto M, Aiba A, Kasuga M, and Kido Y**. Ras-related C3 botulinum toxin substrate 1 (RAC1) regulates glucose-stimulated insulin secretion via modulation of F-actin. *Diabetologia* 56: 1088-1097, 2013.

65. **Wang Z, Oh E, Clapp DW, Chernoff J, and Thurmond DC**. Inhibition or ablation of p21-activated kinase (PAK1) disrupts glucose homeostatic mechanisms in vivo. *J Biol Chem* 286: 41359-41367, 2011.

66. **He Y, Li D, Cook SL, Yoon MS, Kapoor A, Rao CV, Kenis PJ, Chen J, and Wang F**. Mammalian target of rapamycin and Rictor control neutrophil chemotaxis by regulating Rac/Cdc42 activity and the actin cytoskeleton. *Molecular biology of the cell* 24: 3369-3380, 2013.

67. **Agarwal NK, Chen CH, Cho H, Boulbes DR, Spooner E, and Sarbassov DD**. Rictor regulates cell migration by suppressing RhoGDI2. *Oncogene* 2012.

638 68. **Wang Z, and Thurmond DC**. Differential phosphorylation of RhoGDI mediates
639 the distinct cycling of Cdc42 and Rac1 to regulate second-phase insulin secretion. *J Biol*
640 *Chem* 285: 6186-6197, 2010.

641 **Figure Legends**

642 **Figure 1. AKT signaling pathway proteins in βRicKO mice islets.** Representative
643 immunoblots of *Control (Ctrl)* and *βRicKO* islets lysates. **A-D)** Quantification of immunoblots
644 of *Ctrl* (white bars) and *βRicKO* (red bars) islets lysates. Data are represented as mean ± SEM (n
645 = 4), **P* < 0.05.

646 **Figure 2. *βRicKO* mice are glucose intolerant due to impaired insulin secretion. A-C)** Body
647 weight, fasting and random fed blood glucose, and plasma insulin in 12-week-old Control (*Ctrl)*
648 and *βRicKO* mice. **D and E)** Intraperitoneal glucose tolerance test and quantification of area
649 under the curve of IPGTT plot in *Ctrl* (black circles) and *βRicKO* (red squares) mice. **F)**
650 Glucose-stimulated insulin secretion in *Ctrl* and *βRicKO* mice. **G**) Insulin tolerance test in *Ctrl*
651 (black circles) and *βRicKO* (red squares) mice. **H)** β-cell mass of *Ctrl* and *βRicKO* mice. Data
652 are represented as mean ± SEM (n ≥ 5), **P* < 0.05.

653 **Figure 3. Mice with tamoxifen inducible post-developmental deletion of Rictor are also**
654 **intolerant to glucose. A and B)** Intraperitoneal glucose tolerance test and quantification of area
655 under the curve of IPGTT plot in tamoxifen-injected *Rictor$^{f/f}$* and *MIP-Cre;Rictor$^{f/f}$* mice. **C)**
656 glucose-stimulated insulin secretion in tamoxifen-injected *Rictor$^{f/f}$* and *MIP-Cre;Rictor$^{f/f}$* mice. **D**
657 **and E)** Assessment of fasting and fed blood glucose and plasma insulin levels in tamoxifen-
658 injected *Rictor$^{f/f}$* and *MIP-Cre;Rictor$^{f/f}$* mice. **F)** β-cell mass of tamoxifen-injected *Rictor$^{f/f}$* and
659 *MIP-Cre;Rictor$^{f/f}$* mice. Data are represented as mean ± SEM (n ≥ 4), **P* < 0.05.

Figure 4. Insulin secretion and actin remodeling are disrupted in β-cells of *βRicKO* mice. A) Glucose- and potassium chloride-stimulated insulin secretion determined by static incubation of islets isolated from *Ctrl* and *βRicKO* mice. LG=3 mM, HG=24mM, Diazoxide=200μM and KCl=30mM. **B)** Insulin content and **C)** ATP/ADP ratio of islets isolated from *Ctrl* and *βRicKO* mice. **D)** Immunoblot and quantification of glucose-induced changes in soluble (G-Actin) and insoluble (F-Actin) in MIN6 cells following treatment with glucose with and without treatment with Torin. **E)** Immunoblot and quantification of soluble (G-Actin) and insoluble (F-Actin) in islets isolated from Control (*Ctrl*) and *βRicKO* mice. **F)** Insulin secretion from islets isolated from *Ctrl* and *βRicKO* mice following treatment with glucose and jasplakinolide. LG=3 mM and HG=24mM. Data are represented as mean ± SEM (n ≥ 3), **P* < 0.05, ****P* < 0.001 and *****P* < 0.0001.

Figure 5. Incretin action ameliorates glucose intolerance of *βRicKO* mice. Glucose tolerance test, quantification of area under the curve of IPGTT plot and oral glucose-stimulated insulin secretion following oral glucose tolerance test (A-C), intraperitoneal glucose tolerance test with co-administration of GLP-1 (D-F) and GIP (G-I) in *Ctrl* and *βRicKO* mice. Data are represented as mean ± SEM (n ≥ 7), **P* < 0.05.

Figure 6. Glucagon-like peptide 1 modulates actin remodeling and insulin granule dynamic in β-cells. A) Insulin secretion from islets isolated from Control (*Ctrl*) and *βRicKO* mice following treatment with glucose and GLP-1. LG=3 mM and HG=24mM. **B)** Immunoblot and quantification of glucose-induced changes in soluble (G-Actin) and insoluble (F-Actin) in islets isolated from *Ctrl* and *βRicKO* mice following treatment with glucose and GLP-1. LG=3 mM and HG=24mM. **C)** Immunoblot and quantification of glucose-induced changes in soluble (G-Actin) and insoluble (F-Actin) in MIN6 cells following treatment with glucose with and GLP-1.

683 *$P < 0.05$ HG vs LG within group and # $P < 0.05$ between groups HG Ctrl vs HG and & $P <$

684 0.05 within group HG βRicKO vs HG+GLP-1 βRicKO. **D)** Quantification of insulin granules

685 movement (distance/time) in MIN6 cells with and without administration of Torin and/or GLP-1.

686 HG=24mM. Data are represented as mean ± SEM (n≥4), *$P < 0.05$ and **$P < 0.01$.

Figure 1

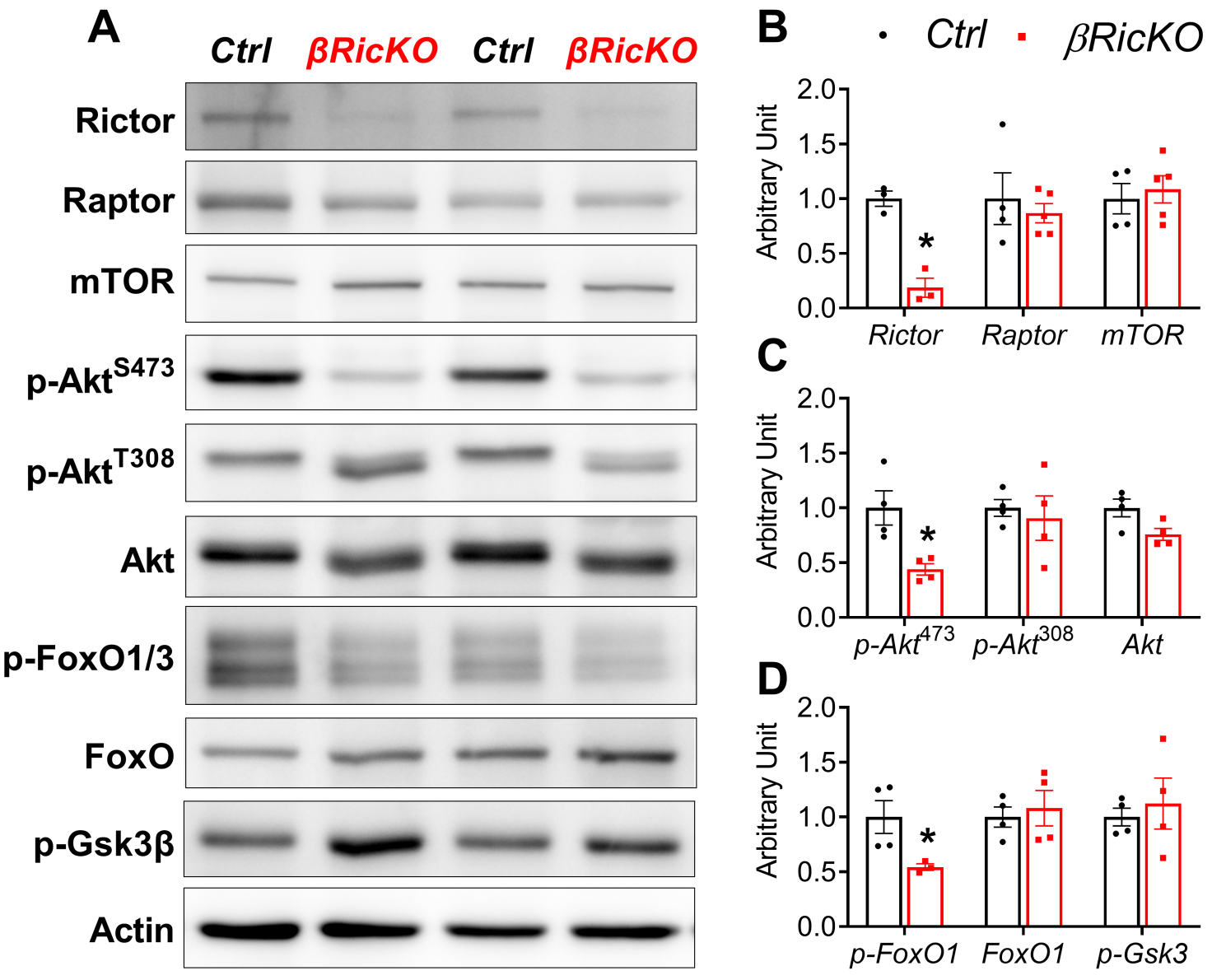
A
Ctrl
βRicKO
Ctrl
βRicKO
Rictor
Raptor
mTOR
p-Akt S473
p-Akt T308
Akt
p-FoxO1/3
FoxO
p-Gsk3β
Actin
B
Ctrl
βRicKO
Arbitrary Unit
2.0
1.5
1.0
0.5
0.0
*
Rictor
Raptor
mTOR
C
Arbitrary Unit
2.0
1.5
1.0
0.5
0.0
*
p-Akt473
p-Akt308
Akt
D
Arbitrary Unit
2.0
1.5
1.0
0.5
0.0
*
p-FoxO1
FoxO1
p-Gsk3

Figure 2

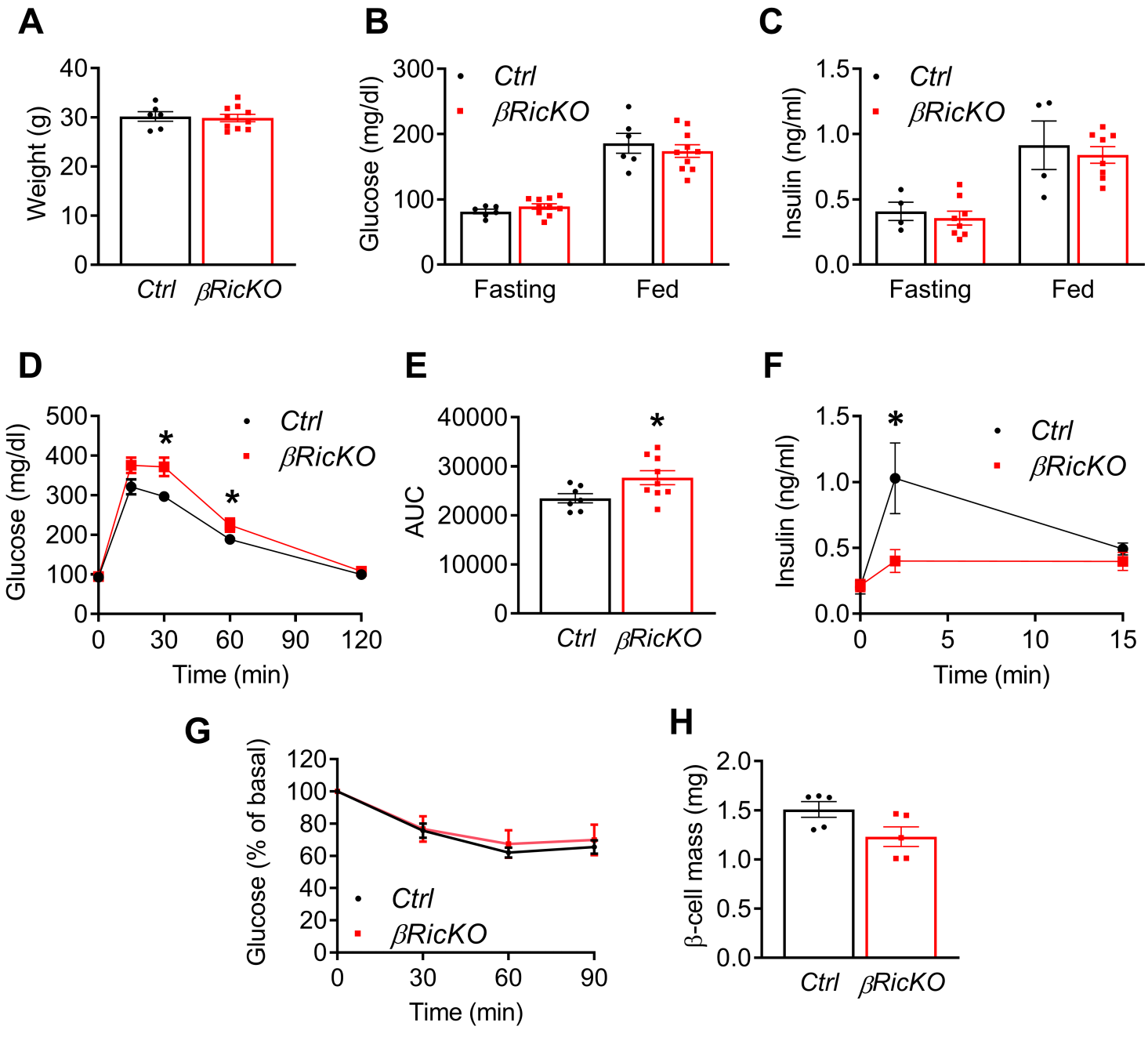
A
Weight (g)
40
30
20
10
0
Ctrl
βRicKO
B
Glucose (mg/dl)
300
200
100
0
Ctrl
βRicKO
Fasting
Fed
C
Insulin (ng/ml)
1.5
1.0
0.5
0.0
Ctrl
βRicKO
Fasting
Fed
D
Glucose (mg/dl)
500
400
300
200
100
0
*
*
Ctrl
βRicKO
0
30
60
90
120
Time (min)
E
AUC
40000
30000
20000
10000
0
*
Ctrl
βRicKO
F
Insulin (ng/ml)
1.5
1.0
0.5
0.0
*
Ctrl
βRicKO
0
5
10
15
Time (min)
G
Glucose (% of basal)
120
100
80
60
40
20
0
Ctrl
βRicKO
0
30
60
90
Time (min)
H
β-cell mass (mg)
2.0
1.5
1.0
0.5
0.0
Ctrl
βRicKO

Figure 3

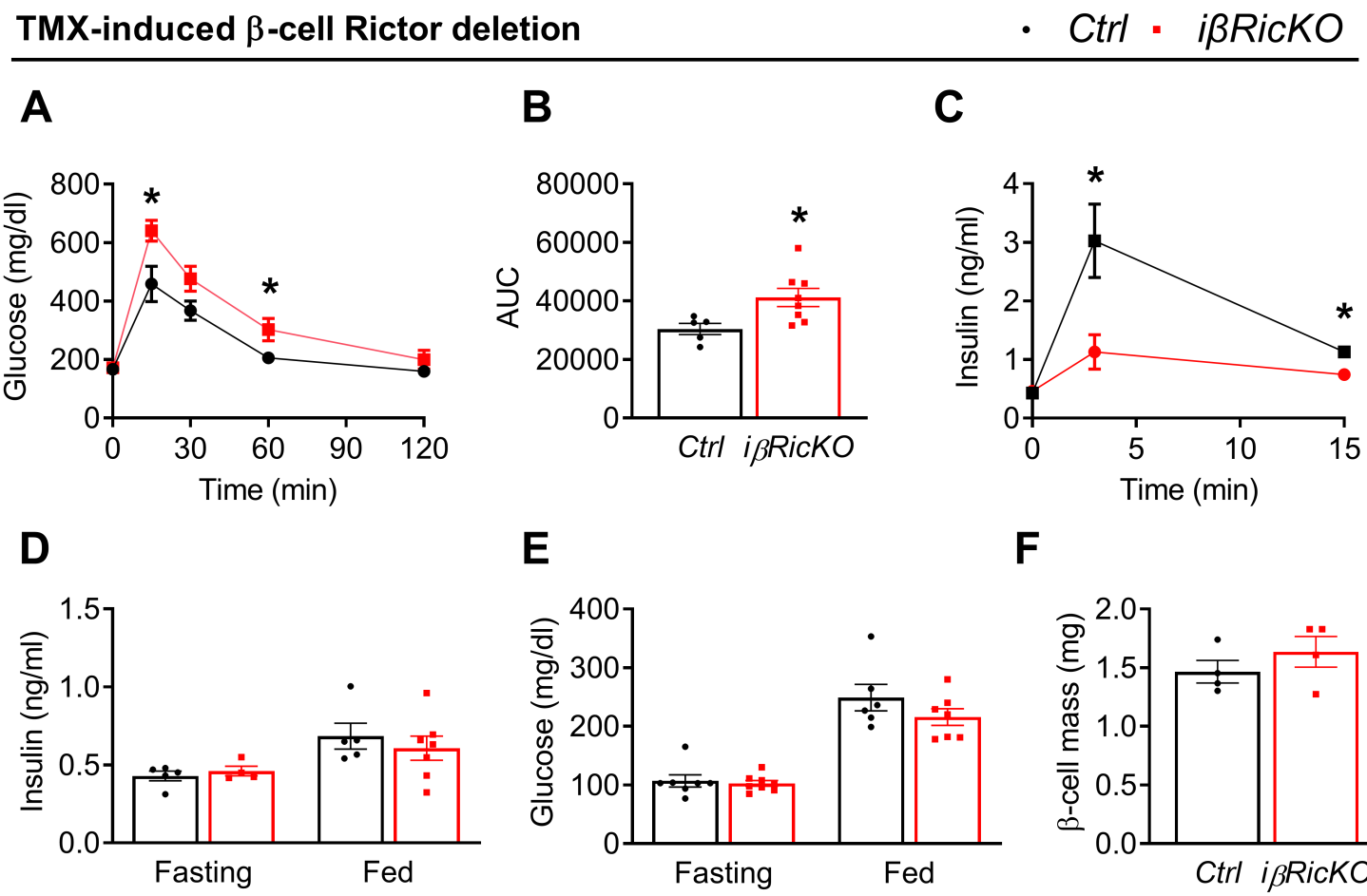
TMX-induced β-cell Rictor deletion
Ctrl
iβRicKO
A
Glucose (mg/dl)
Time (min)
B
AUC
Ctrl
iβRicKO
C
Insulin (ng/ml)
Time (min)
D
Insulin (ng/ml)
Fasting
Fed
E
Glucose (mg/dl)
Fasting
Fed
F
β-cell mass (mg)
Ctrl
iβRicKO

Figure 4

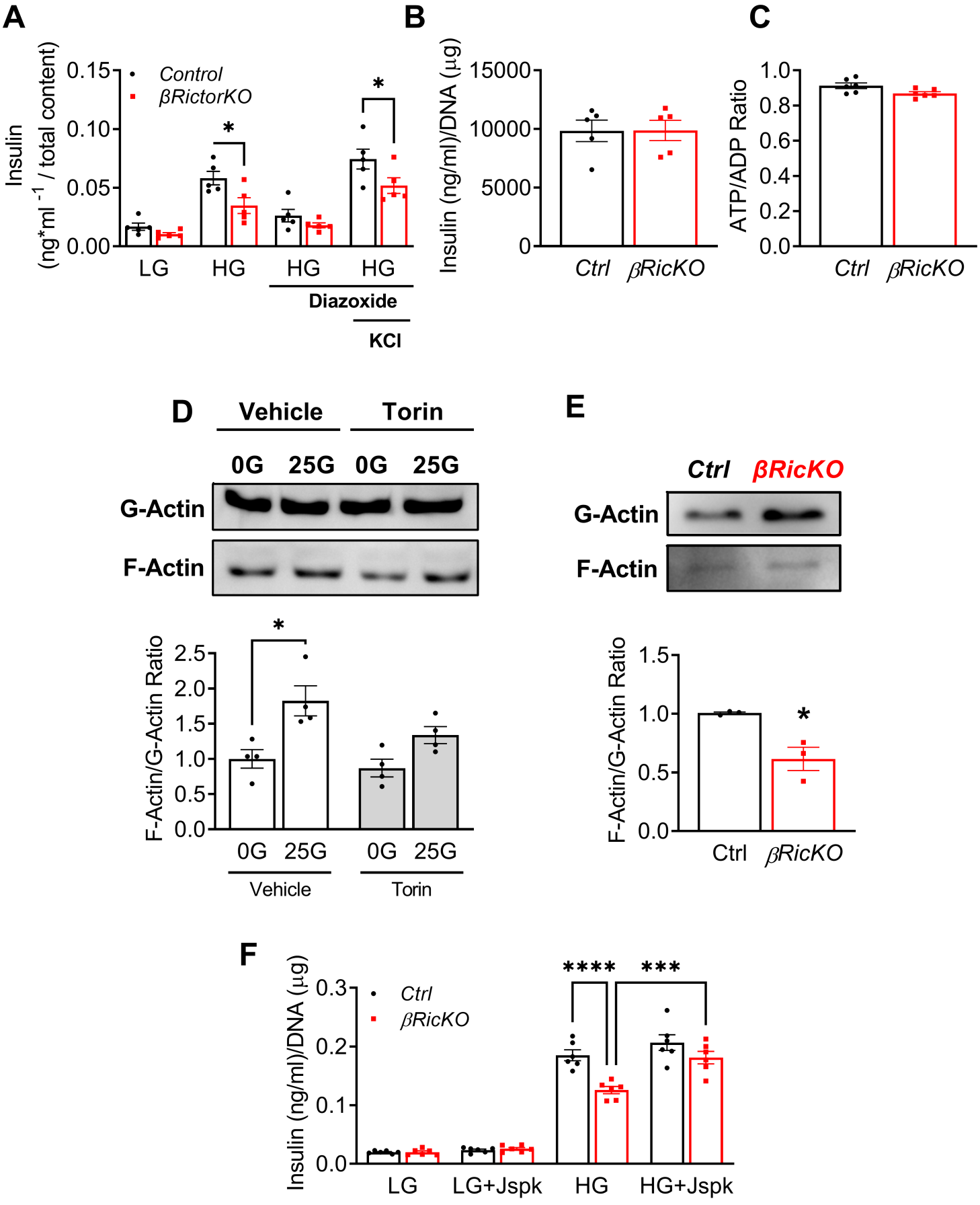
A
Insulin (ng*ml -1 / total content)
0.15
0.10
0.05
0.00
Control
βRictorKO
*
*
LG
HG
HG
HG
Diazoxide
KCl
B
Insulin (ng/ml)/DNA (μg)
15000
10000
5000
0
Ctrl
βRicKO
C
ATP/ADP Ratio
1.0
0.8
0.6
0.4
0.2
0.0
Ctrl
βRicKO
D
Vehicle
Torin
0G
25G
0G
25G
G-Actin
F-Actin
F-Actin/G-Actin Ratio
2.5
2.0
1.5
1.0
0.5
0.0
*
0G
25G
0G
25G
Vehicle
Torin
E
Ctrl
βRicKO
G-Actin
F-Actin
F-Actin/G-Actin Ratio
1.5
1.0
0.5
0.0
*
Ctrl
βRicKO
F
Insulin (ng/ml)/DNA (μg)
0.3
0.2
0.1
0.0
Ctrl
βRicKO
****
***
LG
LG+Jspk
HG
HG+Jspk

Figure 5

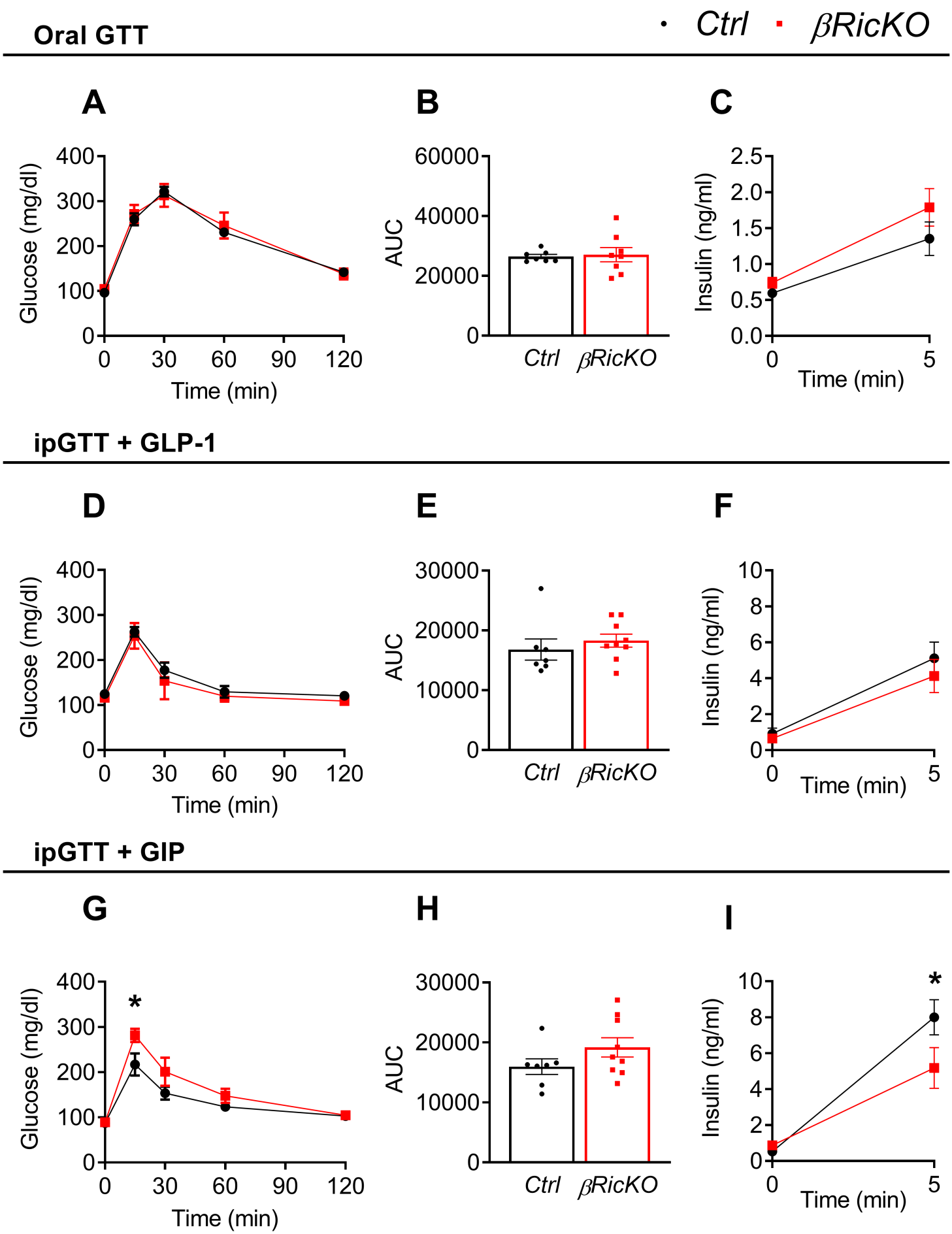
Oral GTT
Ctrl
βRicKO
A
B
C
Glucose (mg/dl)
Time (min)
AUC
Ctrl
βRicKO
Insulin (ng/ml)
Time (min)
ipGTT + GLP-1
D
E
F
Glucose (mg/dl)
Time (min)
AUC
Ctrl
βRicKO
Insulin (ng/ml)
Time (min)
ipGTT + GIP
G
H
I
*
Glucose (mg/dl)
Time (min)
AUC
Ctrl
βRicKO
*
Insulin (ng/ml)
Time (min)

Figure 6

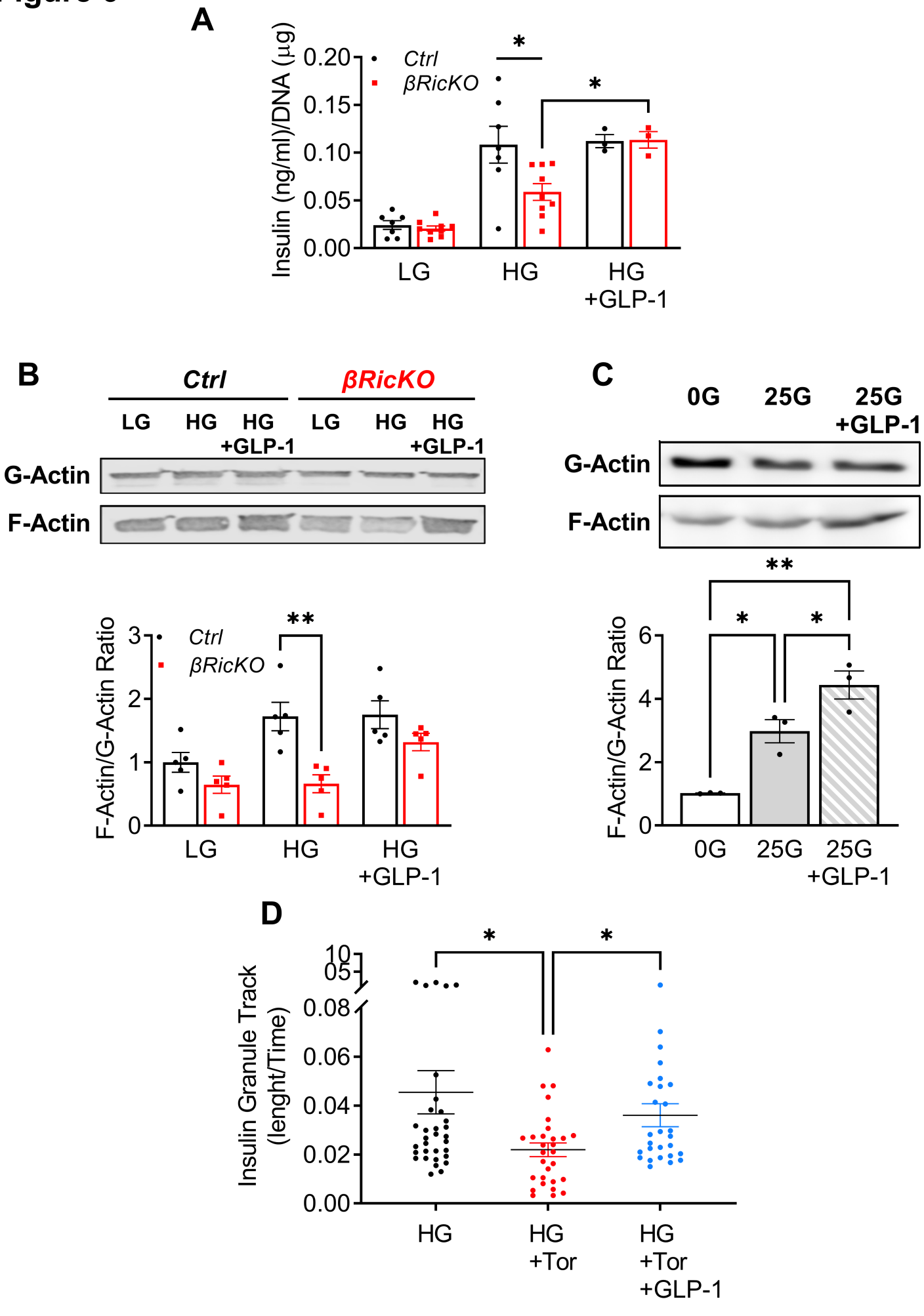
A
Insulin (ng/ml)/DNA (µg)
0.20
0.15
0.10
0.05
0.00
Ctrl
βRicKO
*
*
LG
HG
HG +GLP-1
B
Ctrl
βRicKO
LG
HG
HG +GLP-1
LG
HG
HG +GLP-1
G-Actin
F-Actin
F-Actin/G-Actin Ratio
3
2
1
0
Ctrl
βRicKO
**
LG
HG
HG +GLP-1
C
0G
25G
25G +GLP-1
G-Actin
F-Actin
**
*
*
F-Actin/G-Actin Ratio
6
4
2
0
0G
25G
25G +GLP-1
D
Insulin Granule Track (lenght/Time)
10
05
0.08
0.06
0.04
0.02
0.00
*
*
HG
HG +Tor
HG +Tor +GLP-1

Novel roles of mTORC2 in regulation of insulin secretion by actin filament remodeling

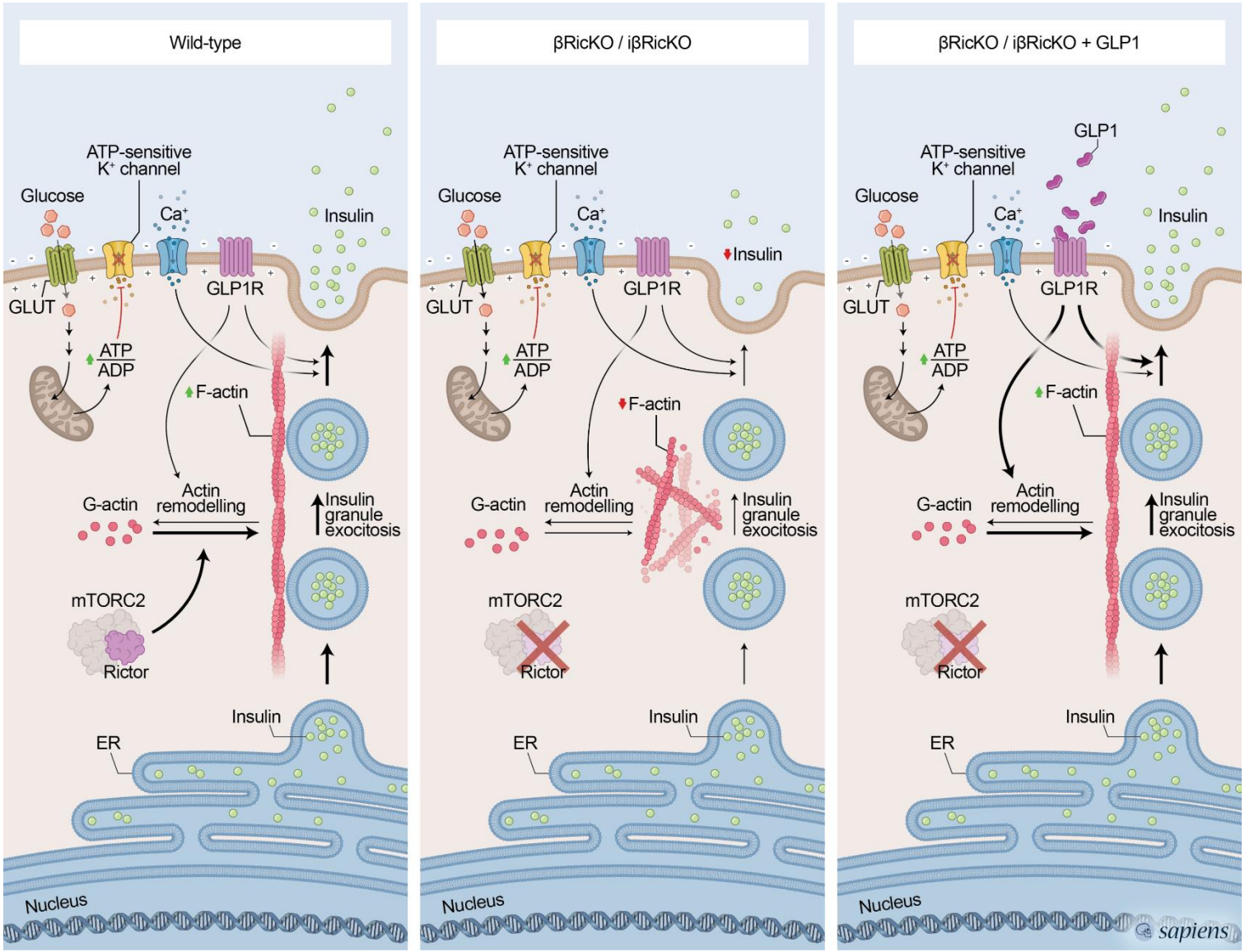

Conclusion: mTORC2 regulates glucose-stimulates insulin secretion by promoting actin filament remodeling. Importantly, GLP-1 rescued defects in insulin secretion by modulating actin polymerization in βRicKO.